

Nesting of electron and hole Fermi surfaces in non-superconducting BaFe₂P₂

B.J. Arnold,¹ S. Kasahara,² A.I. Coldea,^{3,1} T. Terashima,² Y. Matsuda,⁴ T. Shibauchi,⁴ and A. Carrington¹

¹*H. H. Wills Physics Laboratory, University of Bristol, Tyndall Avenue, Bristol, BS8 1TL, United Kingdom.*

²*Research Center for Low Temperature and Materials Sciences, Kyoto University, Sakyo-ku, Kyoto 606-8501, Japan.*

³*Clarendon Laboratory, Department of Physics, University of Oxford, Oxford OX1 3PU, United Kingdom.*

⁴*Department of Physics, Kyoto University, Sakyo-ku, Kyoto 606-8502, Japan.*

We report detailed measurements of the de Haas-van Alphen (dHvA) effect in BaFe₂P₂ which is the end member of the superconducting series, BaFe₂(As_{1-x}P_x)₂. Using high purity samples we are able to observe dHvA oscillations from all the sheets of Fermi surface and hence build up a complete detailed picture of its structure. The results show the existence of a highly warped section of hole surface which may be the origin of the nodal gap structure in this series. Importantly, we find that, even for this non-superconducting end member, one of the hole surfaces almost exactly nests with the inner electron surface. This suggests that improved geometric nesting does not drive the increase in pairing strength with decreasing x in this system.

A common feature that links together the various families of iron-based superconductors is their unusual electronic structure, which consists of almost nested, quasi two dimensional electron and hole Fermi surfaces (FS). This quasi nesting produces strong peaks in the real and imaginary parts of the susceptibility (both bare and interacting), which in many theories [1, 2] drives the superconductivity via a spin-fluctuation mechanism. However, the relative importance of geometric nesting and the many-body interactions (U and J in Hubbard type models) remains under debate. Studies of how the FS evolves and correlates with the changing material properties over the phase diagram are therefore of great importance.

Although, quasi nested electron and hole bands are a common feature of calculated band-structures of these compounds, the exact topology and size of the FS is very difficult to compute from first principles. There are usually four or five bands which cross the Fermi energy, giving rise to small Fermi pockets each of which fills $\sim 10 - 20\%$ of the Brillouin zone volume. The small size of these pockets means their size and topology are very sensitive to small shifts in the band energies, which can result from small structural changes or from interactions with spin-fluctuations which scatter electrons between the electron and hole sheets [3]. Hence, it is important to experimentally determine the full three dimensional FS so that quantitative tests of the theory can be made. Measurements of the de Haas-van Alphen (dHvA) effect provide a very accurate way of measuring the bulk FS.

A particularly useful system for studying the influence of FS topology on the ground state of the iron-based superconductors is BaFe₂(As_{1-x}P_x)₂. Here, the Néel temperature of spin density wave ground state of the end member BaFe₂As₂ is driven to zero and superconductivity emerges with a maximum $T_c = 30$ K, as As is substituted with the isovalent element P. So unlike charge doped iron-pnictide systems, (e.g., Ba_{1-x}K_xFe₂As₂), BaFe₂(As_{1-x}P_x)₂ is expected to remain perfectly com-

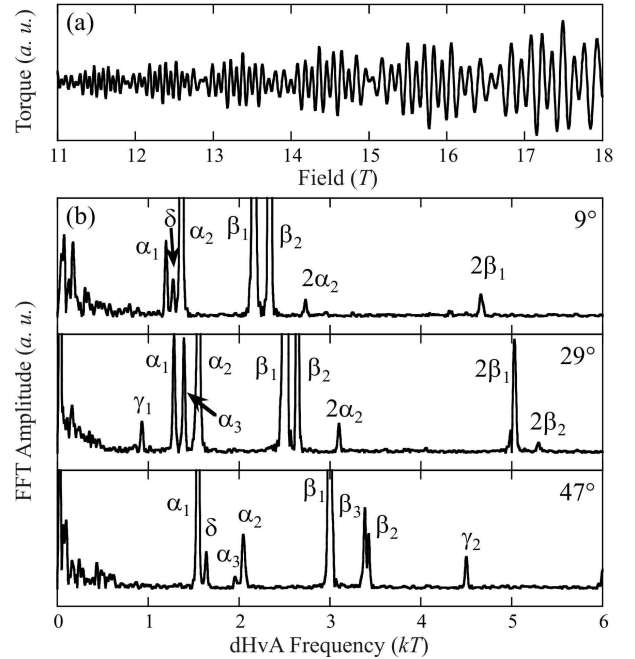


FIG. 1. (a) An example torque versus field trace with background subtracted (b) Fast Fourier transforms of the $\tau(H)$ data (from 6-18 T) at various angles showing the distinct dHvA peaks. Harmonics are identified with the prefix 2. All data was taken at base temperature $T \simeq 0.35$ K. Note the peaks below 0.5 kT are due to noise and features in the background cantilever magnetoresistance.

pensated (equal volumes of electron and hole pockets) for all x . Minimal disorder is introduced in the Fe plane by these substitutions so that dHvA oscillations can be observed over a wide range of x ($0.42 < x \leq 1$) [4].

Structurally, increasing x results in a decrease in the c/a ratio and a movement of the pnictogen atom towards the Fe plane. Density functional theory (DFT) calculations based on the local density approximation (and its

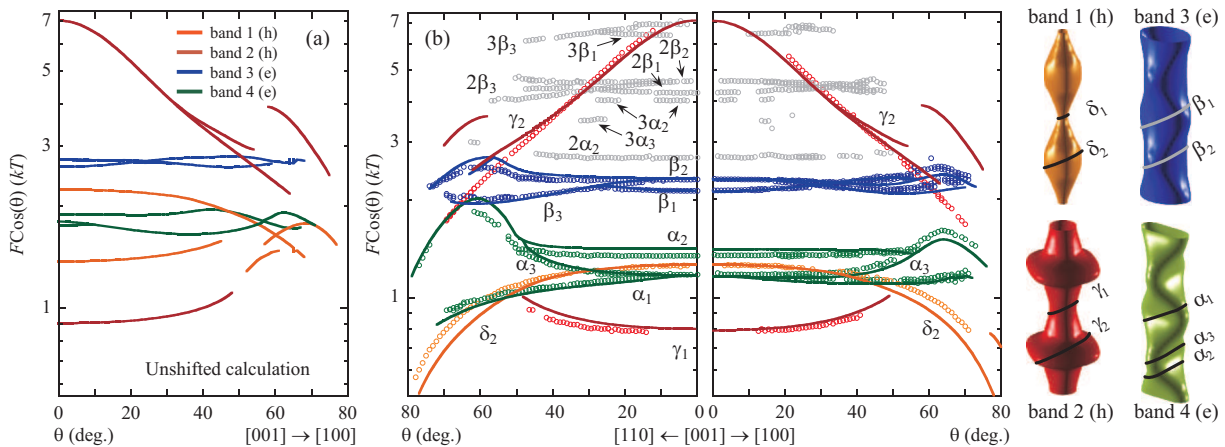


FIG. 2. (color online) dHvA frequencies multiplied by cosine of the rotation angle versus angle. (a) Shows the calculations for the unshifted bands rotating from [001] towards [100]. In (b) the symbols show experimental data for rotations from [001] to both [100] and [110] whereas the solid lines show the calculations for the energy shifted bands as described in the text (note that the predicted orbit δ_1 which has $F \simeq 100$ T at $\theta = 0^\circ$ is not shown) [5]. (c) Shows the origin of the orbits on the calculated electron (e) and hole (h) FS sheets at an angle of $\theta = 20^\circ$ (towards [110]).

variants) predict that throughout the series the electron sheets change very little, but for the hole sheets there are much greater changes [4]. BaFe_2As_2 has three quasi 2D hole sheets but for BaFe_2P_2 one of these disappears and one of the hole sheets develops pronounced warping close to the top of the zone (dumbbell, band 2 in Fig. 2). A notable property of the $\text{BaFe}_2(\text{As}_{1-x}\text{P}_x)_2$ series is that there is clear evidence from multiple probes [6, 7] that there are line nodes in its superconducting energy gap. It has been proposed theoretically that these nodes are located on the dumbbell hole surface [8] although there is experimental evidence that rather points to the nodes being located on the electron sheets [9, 10]. Establishing a clear connection between the unusual gap structure of $\text{BaFe}_2(\text{As}_{1-x}\text{P}_x)_2$ and its FS topology would be a strong confirmation that the pairing mechanism is indeed mediated by spin-fluctuations in these materials.

In previous studies, dHvA signals from *all* of the FS sheets were not observed and so the complete topology could not be determined. In particular, Shishido *et al.* [4] only observed signals from the electron sheets. Following this, Analytis *et al.* [11] reported measurements for $x = 0.63$ where orbits on the smaller hole sheet were observed and were found to correspond to almost the same cross-sectional area as the smaller electron pocket.

Here we report new measurements of the dHvA effect for the end member BaFe_2P_2 . The much higher purity level of our new samples allows us to observe dHvA oscillations originating from all the FS sheets and hence we are able to make a precise determination of the complete FS. A surprising aspect of the results is that they show that even for this non-superconducting (and non-magnetically ordered) composition, one of the hole sheets is almost perfectly nested with the (smaller) electron FS,

similar to that found for the superconducting composition $x = 0.63$ [11]. This suggests that nesting is probably a necessary but not sufficient ingredient for superconductivity.

Samples of BaFe_2P_2 were grown as described in Ref. [12]. The lattice parameters and the crystal orientation was determined by x-ray diffraction. The best results were obtained on a sample with dimensions $50 \times 75 \times 20 \mu\text{m}$, which was mounted on micro piezo resistive cantilever in order to measure the magnetic torque. The torque sensor was fixed to a rotating probe, inside a ^3He cryostat equipped with a superconducting magnet. The orientation of the sample on the cantilever was determined by comparing optical images of the mounted sample with images taken on the x-ray mount. We estimate the accuracy of the in-plane alignment ϕ is around $\pm 5^\circ$.

Example torque τ versus field H data is shown in Fig. 1. In this sample, the oscillations are visible down to fields as low as 5 T at some angles. By taking fast Fourier transforms of the $\tau(B^{-1})$ data we identified 8 different dHvA orbits. As many of these peaks are very close in frequency they can only be clearly identified by performing long field sweeps (typically between 6 and 18 T) with small (1 degree) angular increments. In this way the various crossing branches can be easily identified. Complete rotations were performed in two principle directions, namely from H perpendicular to the Fe plane [001] towards either the [100] or [110] directions. In both cases we define the rotation angle $\theta = 0$ for $H \parallel [001]$.

For a perfectly two dimensional FS sheet, the dHvA frequency $F \propto 1/\cos(\theta)$, hence for quasi-two dimensional systems the dHvA data are best appreciated by plotting $F \cos \theta$ versus θ as in Fig. 2. In such a plot, a local minimum in the FS cross-section (neck) gives rise to a

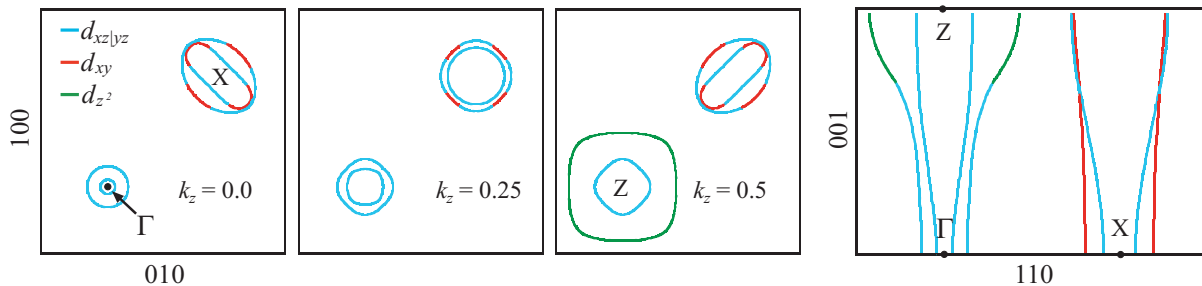


FIG. 3. (color online) Crosssections of the determined Fermi surface of BaFe₂P₂ in: (a) the ab plane at three different k_z values (quoted in units of c^*), (b) a c -axis cut along the [110] direction and through the Γ point. The largest band character element at each \mathbf{k} -point is indicated [13].

branch where $F \cos \theta$ increases with θ , whereas for a local maximum (belly) $F \cos \theta$ decreases with θ .

In order to make a more precise analysis of the results we compare the data with predicted extremal orbits derived from bandstructure calculations. These density functional calculations were done using an augmented plane wave plus local orbitals scheme as implemented in the Wien2K package [14, 15]. The calculated extremal orbits as function of the field angle for a [001] to [100] rotation are shown in Fig. 2(a). Although this calculation reproduces the general features of the experiment, the exact topology and FS size is not well reproduced. As we have found in other pnictide systems [16, 17] the calculation can be brought into much better agreement with experiment by performing rigid (\mathbf{k} -independent) shifts of the band energies. The two electron bands (4 and 3) are easily identified as the α and β branches respectively and these are brought into almost exact agreement by shifting the energies of band 4 up by 68 meV and band 3 up by 58 meV. These surfaces have quite a complicated topology which is well reproduced in the calculations [see Fig. 2(b)]. Note the large differences between the rotation toward [100] and [110]. The large (highest fundamental frequency) orbit γ_2 originates from the highly warped part of the band 2 hole ‘dumbbell’ surface centered around the top of the zone. The calculations reproduce this branch without *any* applied energy shift. The curvature of $F \cos(\theta)$ for the δ_2 branch clearly identifies it as a maximum (belly) crosssection and so it must originate from band 1 as this is the only remain unidentified *maximal* orbit. Shifting the energy of this band down by 113 meV gives an almost exact match. With this shift, the minimal crosssection δ_1 of this band would give a dHvA frequency around 100 T. We do not see conclusive evidence for this orbit probably because its expected weak signal is likely buried in the low frequency cantilever noise (see Fig. 1). Finally, we can identify the last branch γ_1 , as the minimum of band 2. Although no energy shift was required to explain the maximum of this band, we require a shift down of 52 meV to fit the minimum. With these energy shifts, the FS is accurately

TABLE I. Measured effective masses m^* (uncertainty $\sim 2\%$) along with mass enhancements m^*/m_b calculated using the bandstructure values (m_b) from the energy shifted bands. The mean free paths ℓ are also reported [19].

	γ_1	γ_2	δ	α_1	α_2	β_1	β_2
θ	28°	46°	12°	12°	12°	12°	12°
m^*/m_e	2.30	3.32	1.64	1.75	1.58	1.65	1.54
m^*/m_b	1.59	1.59	1.80	1.82	1.88	1.68	1.81
ℓ (nm)	40	150	40	190	200	170	160

determined. As a check we calculate the number of electron and holes in each shifted FS sheet and find that, as expected, they are equal to within 0.017 electrons per unit cell.

It has been suggested that physically these shifts result from a spin fluctuation interaction [3]. Scattering of electrons by the spin-fluctuations between the electron and hole surfaces causes both surfaces to shrink in volume and hence the energy shifts are in opposite directions. This is supported by results for CaFe₂P₂ [18], which has a non-nested FS similar to the collapsed tetragonal, high pressure phase of CaFe₂As₂, and where the DFT calculations are in excellent agreement with experiment without any shifting. Further, for BaFe₂(As_{1-x}P_x)₂ it was found that the size of energy shifts varied approximately linearly with x , becoming larger as the SDW phase transition is approached [4] and the spin-fluctuations grow in magnitude. Our results here also support this interpretation, because we find that most sections of the FS of BaFe₂P₂ are close to being geometrically nested and are smaller compared to the DFT calculation whereas the highly warped part of band 2 dumbbell (γ_2 orbit) is far from nesting and remains unchanged. This supports the suggestion of Suzuki *et al.* [8] that this part of the Fermi surface does not contribute strongly to the pairing and is therefore may be susceptible to gap node formation.

The masses m^* of the quasiparticles on each of the extremal orbits were determined by measuring the temperature dependence of the dHvA oscillation amplitude

[19]. Fits to this data to determine m^* are reported in Table. I, along with the masses m_b calculated from the shifted band-structure bands for the same orbits and at the same field angles. The mass enhancements m^*/m_b are all relatively similar and small ranging from 1.6 to 1.9. Note the values for the β orbits are smaller than the value give in Ref. [4] but consistent within the error.

An interesting feature of the results is that they show that for this non-superconducting end member of the $\text{BaFe}_2(\text{As}_{1-x}\text{P}_x)_2$ series, one of the electron and hole sheets are very well nested. The closeness of the cross-sectional areas of the inner electron and hole FS is evident from the rotation plots shown in Fig. 2. The fact that these areas are so close explains why they were not observed in previous studies, where the dHvA oscillations were not observable over such a wide range of inverse field as that were here. In Fig. 3 we show sections through the determined FS. Although the in-plane area of the electron sheet FS does not change strongly with k_z , its shape does. Because of the symmetry of the body centered tetragonal unit cell the crosssection at the zone center is exactly the same as at the zone top but rotated by $\pi/2$. The best match, where the inner electron sheet is almost perfectly circular is half way between these points at $k_z = 0.25$. Furthermore the band character of these two sheets is also very similar; they both have predominantly Fe $d_{xz/yz}$ character.

Comparing our data with that of Analytis *et al.*[11] for the superconducting ($T_c = 7\text{K}$) composition $x = 0.63$ suggests that besides the above mentioned shrinking of the overall size of the Fermi surface there is remarkably little change in the overall topology with x (for $0.63 \leq x \leq 1$). A close comparison between the two data sets [19] shows that the $F(\theta)$ data may be almost perfectly superimposed by simply scaling the mean frequencies of the electron bands. This suggests that the c -axis warping of the electron and hole sheets remain remarkably constant as a function of P content x . The anomalous downturn in the frequency of the electron α branch between $\theta = 40^\circ$ and 50° identified in Ref. [11] was correctly assigned to a crossing of the hole and electron orbit frequencies. However, the higher scattering in these doped samples probably prevented the observation of the dumbbell (γ_2) orbit. In Ref. [11] the γ branch was assigned to the minimum of band 1. However, as the size and dispersion of this branch is almost identical to the γ_1 branch in the present work we suggest that this assignment was incorrect, and it is instead the minimum of band 2 as in the present work. This effects somewhat the fitted band structure of Ref. [11] but does not change the conclusion that the electron and hole bands are well nested for $x = 0.63$.

Combined with the present results it appears then that rather than the bands become much better nested as x approaches that optimal for superconductivity, the *relative* size of the electron and hole sheets remain remark-

ably constant. As the electron sheets shrink with decreasing x the hole bands shrink by a similar amount without any major change in topology. This is not expected from conventional bandstructure calculations, where the hole band topology changes very dramatically as x is decreased. It is therefore likely that the dumbbell shape of the larger hole band remains for the superconducting compositions. Recent photoemission results for the $x = 0.38$ composition [20] indicate the FS topology of this close to optimal T_c composition is indeed close to that observed here for the end member.

In summary, our results determine, in very high detail, the structure of the FS of the end member of the $\text{BaFe}_2(\text{As}_{1-x}\text{P}_x)_2$ series. Together with the known shrinking of the average size of the electron pockets and invoking the expected compensated nature of the FS, it is now possible to estimate the topology of both the electron and hole surface across the phase diagram. An important aspect of the results is that they show that one of the hole and electron FS are well nested even for this non-superconducting (and non magnetic) composition. This suggests that the increase in pairing susceptibility as x is decreased is caused by increases in the many body interaction parameters U and J rather than any effect of improved geometric nesting.

We thank Mairi Haddow for assistance with the x-ray diffraction measurements and Ed Yelland for the use of computer code. This work was supported by the UK EPSRC and by KAKENHI from JSPS .

-
- [1] I. I. Mazin, D. J. Singh, M. D. Johannes, and M. H. Du, *Phys. Rev. Lett* **101**, 057003 (2008).
 - [2] K. Kuroki, *et al.*, *Phys. Rev. Lett.* **101**, 087004 (2008).
 - [3] L. Ortenzi, E. Cappelluti, L. Benfatto, and L. Pietronero, *Phys. Rev. Lett.* **103**, 046404 (2009).
 - [4] H. Shishido, *et al.*, *Phys. Rev. Lett.* **104**, 057008 (2010).
 - [5] For the calculations of the [001]-[100] rotation we used an in-plane angle of $\phi = 10^\circ$ as this gave the best fit whereas for the [001]-[110] we used exactly $\phi = 45^\circ$.
 - [6] K. Hashimoto, *et al.*, *Phys. Rev. B* **81**, 220501(R) (2010).
 - [7] Y. Nakai, *et al.*, *Phys. Rev. B* **81**, 020503 (2010).
 - [8] K. Suzuki, H. Usui, and K. Kuroki, *J. Phys. Soc. Jpn.* **80**, 013710 (2011), arXiv:1010.3542.
 - [9] K. Hashimoto, *et al.*, *Phys. Rev. B* **82**, 014526 (2010).
 - [10] M. Yamashita, *et al.*, arXiv:1103.0885.
 - [11] J. G. Analytis, J.-H. Chu, R. D. McDonald, S. C. Riggs, and I. R. Fisher, *Phys. Rev. Lett.* **105**, 207004 (2010).
 - [12] S. Kasahara, *et al.*, *Phys. Rev. B* **81**, 184519 (2010).
 - [13] For the outer hole band we smoothly interpolated between the shifted and unshifted Fermi surfaces to give the correct crosssections for the neck and belly orbits of this surface for this figure.
 - [14] P. Blaha, K. Schwarz, G. K. H. Madsen, D. Kvasnicka, and J. Luitz, *WIEN2K, An Augmented Plane Wave + Local Orbitals Program for Calculating Crystal Properties* (Karlheinz Schwarz, Techn. Universität Wien, Austria,

- 2001).
- [15] Using the experimental atomic coordinates, $a=3.840 \text{ \AA}$, $c=12.442 \text{ \AA}$ and $Z_p=0.3456$.
 - [16] A. I. Coldea, *et al.*, Phys. Rev. Lett. **101**, 216402 (2008).
 - [17] J. G. Analytis, *et al.*, Phys. Rev. Lett. **103**, 076401 (2009).
 - [18] A. I. Coldea, *et al.*, Phys. Rev. Lett. **103**, 026404 (2009).
 - [19] See supplementary material at <http://link.aps.org/supplemental/xxx> for details of the effective mass and mean free path determinations and a comparison with the results of Ref. [11].
 - [20] T. Yoshida, *et al.*, Phys. Rev. Lett. **106**, 117001 (2011).